J. Chem. Sci. (2021)133:90
https://doi.org/10.1007/s12039-021-01967-6

REGULAR ARTICLE

Selectivity of diallyl trisulfides (DATS) in reducing $HAuCl_4$ to produce gold nanoparticles: a detailed investigation

NILADRI SEKHAR MANDAL, ARUNAVO CHATTERJEE and PRADIPTA PURKAYASTHA *

Department of Chemical Sciences and Center for Advanced Functional Materials, Indian Institute of Science Education and Research (IISER) Kolkata, Mohanpur 741246, West Bengal, India
E-mail: ppurkayastha@iiserkol.ac.in

MS received 23 April 2021; revised 10 June 2021; accepted 16 June 2021

Abstract. The bulbous root garlic (*Allium sativum*) with a strong taste and pungent odor is used widely in culinary preparations and folk medicine. Silver and gold nanoparticles (NPs) synthesized using this ingredient have also shown medicinal and therapeutic potency. Garlic contains organosulfur compounds, such as diallyl sulfide (DAS), diallyl disulfide (DADS) and diallyl trisulfide (DATS). These compounds are of crucial significance as anticancer drugs. Reported here is a synthesis of a series of DATS with varying substituents and plausible application as capping as well as reducing agent to synthesize gold nanoparticles (TS-GNPs). In the process, it was discovered that among the selected DATs, only 1,3-di(but-1-ene)trisulfane could serve the purpose because of structural reasons. The reason for this intriguing selectivity has been investigated in detail using the experimental findings and theoretical calculations of the frontier molecular orbitals (FMO).

Keywords. Trisulfide ligands; Gold nanoparticles; Protecting ligand; Reducing agent; Selectivity.

1. Introduction

Nanoscience and nanotechnology are contributing enormously to the advancement of modern-day research in developing various sensors and catalysts, and in biomedical research, information technologies and electronics.[1–5] Worldwide research in the area of biomaterials is overwhelmed by the works on metal nanoparticles (NPs) in recent years due to the inventions of various methods of synthesis and characterization.[6,7] In this regard, gold nanoparticles (GNPs) have attracted wide attention due to their potency in biology, catalysis, electrical conductivity, optical properties, etc. depending on their size and shape.[8,9] Proliferating success is achieved by engineering the NPs to function in effective and targeted drug delivery aiming towards *in vitro* diagnostics, prosthetic implants, bio-designing, bio-imaging and therapies.[10–12] Additionally, GNPs have a strong binding affinity towards thiols, disulfides, trisulfides and amines (due to soft-soft interaction resulting in the formation of partial covalent bond) that facilitates its conjugation with DNA, proteins, bio-receptors, etc.[13–19] Surface plasmon enhanced absorption and scattering in GNPs contribute to their unique physicochemical properties[20,21] making them important for bio-imaging and therapeutics.[22,23] Moreover, GNPs are not susceptible to photobleaching and very compatible with human cells.

Plant extracts are frequently used nowadays to synthesize metal NPs. One such important botanical source to synthesize metal NPs is garlic (*Allium sativum*). Several reports are there in the literature on the use of garlic extract to synthesize silver NPs (SNPs) from $AgNO_3$.[24–27] Garlic extract is well known for its medicinal importance due to its applications as antiparasitic, anticancer, antiseptic and antibacterial agents. The active medicinal ingredient in crushed garlic is allicin, which is the most abundant thisulfinate.[28] Similarly, GNPs were also synthesized using garlic extract.[29,30] Such GNPs were reportedly hepatoprotective, antiviral and possess urease, xanthine oxidase and carbonic anhydrase inhibitory activity. The active ingredients in garlic, such as the

*For correspondence

Supplementary Information: The online version contains supplementary material available at https://doi.org/10.1007/s12039-021-01967-6.

Published online: 03 September 2021

polyphenols and terpenoids, were phytochemically determined and the synthesized GNPs were protected by phenolic and organosulfur compounds, amino acids, carboxylic groups and proteins.[31,32] Rastogi and Arunachalam reported two types of organosulfur compounds in garlic extract.[30] The first group contains lipid-soluble diallyl sulfide, diallyl disulfide (DADS) and diallyl trisulfide (DATS) and the second group consists of water-soluble sallylcysteine (SAC) and sallylmercaptocycsteine (SAMC). This report also discussed the molecular basis for the formation of GNPs using the water-soluble variety of the organosulfurs.

So far, the synthesis and applications of SNPs and GNPs from garlic extract were restricted mostly to the medicinal activity without going deep into the molecular structural details. The lipid-soluble DADS and DATS remained untouched in this respect and there is hardly any report on their molecular mechanism in the literature. Since the biological cell membranes are constructed of lipid bilayer, DADS and DATS would be easily accepted by the cells to execute their medicinal properties. We synthesized stable GNPs using DATS as the reducing as well as the protecting agent. We also considered the DATS-mediated production of the reactive oxygen species (ROS) which serve as cancer cell killer without any harmful side effects. In the process, we discovered that only one variety of DATS, 1,3-di(but-1-ene)trisulfane, could selectively construct the GNPs due to its structural peculiarity and the mode of distribution of electrons in the molecular orbitals.

2. Experimental

2.1 *Materials*

All the halides, namely, (1) n-propyl bromide, (2) bromo-2-methylpropyl, (3) 4 -bromo-1-butene, (4) 3-bromoprop-1-ene, (5) benzyl bromide, (6) 4-chloro benzyl chloride, (7) 4-cyano benzyl chloride and sodium thiosulfate, sodium sulfide, stannous chloride dihydrate, sulfur powder and cupric chloride were purchased from SRL Chemicals. Chloroauric acid (gold salt) was purchased from Sigma Aldrich. The solvents were procured from Merck, India.

2.2 *General synthesis of the trisulfides*

To the saturated aqueous solution of sodium thiosulfate $Na_2S_2O_3{\cdot}5H_2O$, 1.3 equiv.), the corresponding unsaturated alkyl bromide (R-X, 1 equiv.) was added dropwise at 50–60 °C with stirring. The reaction mixture was allowed to cool down to room temperature when the solution turned clear. Solution of sodium sulfide ($Na_2S{\cdot}5H_2O$, 1 equiv.) was added to the cooled mixture. The initiation and progress of the reaction were monitored by TLC analysis. Ethyl acetate was used to extract the organic layer. Further, the organic layer was washed with brine solution and dried over anhydrous sodium sulfate. The solvents were evaporated to obtain the desired product mixture which was further purified by column chromatography (silica gel 230–400 mesh).

2.2a *Compound 1*: n-propyl bromide (4 mL, 43.9 mM) was added dropwise to the saturated solution of $Na_2S_2O_3{\cdot}5H_2O$ (14.18 gm, 57.15 mM) at 50–60 °C. The solution was stirred with continuous heating until it turned visibly clear. Solution of $Na_2S{\cdot}5H_2O$ (2.21 gm, 13.17 mM) was added to the mixture when it was cooled to room temperature. TLC was checked to monitor the reaction with continuous stirring. The organic layer was extracted with ethyl acetate and washed with brine, and dried over anhydrous sodium sulfate. The product mixture was purified by column chromatography with hexane as eluent. $R_f = 0.909$ (TLC eluted in 100% hexane); yield: 0.66%; ^{1}H NMR: (300 MHz, $CDCl_3$) $\delta = 2.85$–2.84 (d, 4H, $J = 6$ Hz), 1.79–1.76 (t, 4H, $J = 9$ Hz), 1.02–1.01 (d, 6H, $J = 6$ Hz); ^{13}C NMR: ($CDCl_3$) $\delta = 77.46$, 77.25, 77.04, 41.04, 22.35, 13.35; ESI^+-MS (m/z) = 181.006.

2.2b *Compound 2*: 1-bromo-2-methylpropyl (2 mL, 19.08 mM) was added dropwise to the saturated solution of $Na_2S_2O_3{\cdot}5H_2O$ (6.15 gm, 24.81 mM) at 50–60 °C. The solution was stirred with continuous heating until the solution turned visibly clear. Solution of $Na_2S{\cdot}5H_2O$ (0.961 gm, 6.724 mM) was added to the mixture when it was cooled to room temperature. TLC was checked to monitor the reaction with continuous stirring. The organic layer was extracted with ethyl acetate and washed with brine, and dried over anhydrous sodium sulfate. The product mixture was purified by column chromatography with hexane as eluent. $R_f = 0.75$ (TLC eluted in 100% hexane); yield: 13.7%; ^{1}H NMR: (300 MHz, $CDCl_3$) $\delta = 2.77$ (d, 4H), 2.59 (m, 2H), 1.00 (d, 12H); ^{13}C NMR: ($CDCl_3$) $\delta = 48.77$, 28.38, 21.96; ESI^+-MS (m/z) = 207.01.

2.2c *Compound 3*: 4-bromo-1-butene (0.5 mL, 4.925 mM) was added dropwise to the saturated

solution of $Na_2S_2O_3{\cdot}5H_2O$ (1.59 gm, 6.40 mM) at 50–60 °C. The solution was stirred with continuous heating until the solution turned visibly clear. Solution of $Na_2S{\cdot}5H_2O$ (0.248 gm, 1.477 mM) was added to the mixture when it was cooled to room temperature. TLC was checked to monitor the reaction with continuous stirring. Organic layer was extracted with ethyl acetate and washed with brine, and dried over anhydrous sodium sulphate. The product mixture was purified by column chromatography with hexane as eluent. $R_f = 0.727$ (TLC eluted in 100% hexane); yield: 3.1%; ^{1}H NMR: (300 MHz, $CDCl_3$) $\delta = 5.84–5.81$ (m, 1H), 5.13–5.04 (m, 2H), 2.75 (s, 2H), 2.45–2.44 (3H, J = 6 Hz); ^{13}C NMR: ($CDCl_3$) $\delta = 136.41$, 116.49, 38.37, 33.60; ESI$^+$-MS (m/z) = 207.001.

2.2d *Compound 5*: Benzyl bromide (2 mL, 16.37 mM) was added dropwise to the saturated solution of $Na_2S_2O_3{\cdot}5H_2O$ (5.281 gm, 21.2 mM) at 50–60 °C. The solution was stirred with continuous heating until the solution turned visibly clear. Solution of $Na_2S{\cdot}5H_2O$ (0.825 gm, 4.911 mM) was added to the mixture when it was cooled to room temperature. TLC was checked to monitor the reaction with continuous stirring. The organic layer was extracted with ethyl acetate and washed with brine, and dried over anhydrous sodium sulfate. The product mixture was purified by column chromatography with hexane as eluent. $R_f = 0.75$ (TLC eluted in 100% hexane); yield: 28.5%; ^{1}H NMR: (300 MHz, $CDCl_3$) $\delta = 3.60$ (s, 4H), 7.32–7.31 (t, 4H, $J = 6$ Hz), 7.25–7.23 (t, 6H, $J = 6$ Hz); ^{13}C NMR: ($CDCl_3$) $\delta = 137.57$, 129.62, 128.69, 127.63, 43.48; ESI$^+$-MS (m/z) = 279.16.

2.2e *Compound 6*: 4-chloro benzyl chloride (4 mL, 31.27 mM) was added dropwise to the saturated solution of $Na_2S_2O_3{\cdot}5H_2O$ (10.08 gm, 40.651 mM) at 50–60 °C. The solution was stirred with continuous heating until the solution turned visibly clear. Saturated solution of $Na_2S{\cdot}5H_2O$ (0.015 gm 0.09381 mM) was added to the mixture when it was cooled to room temperature. TLC was checked to monitor the reaction with continuous stirring. The organic layer was extracted with ethyl acetate and washed with brine, and dried over anhydrous sodium sulfate. The product mixture was purified by column chromatography with hexane as eluent. $R_f = 0.56$ (TLC eluted in 100% hexane); yield: 1.18%; ^{1}H NMR: (300 MHz, $CDCl_3$) $\delta = 7.29–7.22$ (q, 4H, $J = 6$ Hz), 4.12 (s, 1H), 4.02 (s, 2H), 3.97 (s, 1H); ESI$^+$-MS (m/z) = 344.02.

2.3 *Preparation of trisulfide induced gold nanoparticles (TS-GNPs)*

TS-GNPs were prepared by the addition of different volumes of 50 mM of respective TS derivative compounds in DMSO to 5 mL of 0.01% chloroauric acid under boiling condition (for 5–6 min). TS-GNPs were centrifuged at 13500 rpm for 30 min at room temperature. The precipitate was then washed twice with double distilled autoclaved water by centrifugation as mentioned. The concentration of TS-GNPs were calculated using an established method considering a part of gold from $HAuCl_4$ was reduced by TS compounds during the method of preparation and found to be 73.51 mM.[33,34]

2.3a *Absorption spectral analysis*: Absorption spectra of TS derivative compounds and TS-GNPs were recorded in the wavelength region ranging from 250 nm to 700 nm using a double beam spectrophotometer (U-2900, HITACHI UV-Spectrophotometer).

2.4 *Measurement of particle size and surface charge*

The hydrodynamic diameters of the GNPs were measured by Dynamic Light Scattering (DLS) using Horiba Nanoparticle Analyzer, nanoPartica SZ-100V2. Poly Dispersity Index (PDI) gives the indication of particle size distribution which was calculated as the weight average molecular weight divided by the number average molecular weight. Surface charges of the GNPs were determined by measuring the zeta potential using Horiba Nanoparticle Analyzer, nanoPartica SZ-100V2.

2.5 *TEM analysis*

The TEM images were recorded with a JEOL, JEM-2100F microscope using a 200 kV electron source at the DST-FIST facility in IISER Kolkata. A drop-casted and a dried sample of the TS-GNPs was prepared on a carbon-coated copper grid. Electron dispersive spectroscopy (EDS) was performed using a JEM-2100F field emission gun electron microscope with EDS, diffraction pattern software, and high angle annular dark-field scanning transmission electron microscopy detector.

2.6 *FTIR spectroscopy*

IR spectra were recorded on a Bruker (model ALPHA) FT-IR spectrometer using the attenuated total reflection (ATR) technique in a liquid phase.

3. Results and Discussion

3.1 *Prospect of the DATs toward GNP synthesis*

The toxicity of DATS to carcinogenic cells is well known.[35–37] DATS are reported to be more toxic to prostate cancer cells compared to non-cancerous epithelial cells.[35] In addition, DATS were found to induce apoptosis in primary effusion lymphoma,[36] and inhibit the spreading of primary colorectal cancer cells depending on the administering dose.[37] We synthesized a series of new DATS derivatives by modifying the parent DATS assuming these to preserve the beneficial properties. Based on the DATS and keeping the tri-thio-ether structure unchanged, we introduced allyl/alkyl/benzyl groups. In this way, both the side chains improved the stability of tri-thio-ether by increasing the stereospecific blockade. The introduction of different new groups could increase the hydrophobicity, molecular volume and the reducing capacity of the aggregated gold atoms to synthesize stable GNPs without involving any other stabilizing agents. DATS acts as a ligand aiming to prepare a more efficient anti-proliferative substance. Here, we have synthesized and investigated the effects and the possible functions of DATS derivatives including (1) 1,3-di(n-propyl)trisulfane, (2) 1,3-di(isobutyl)trisulfane, (3) 1,3-di(but-1-ene)trisulfane, (5) 1,3-di(benzyl)trisulfane and (6) 1,3-di(4-chloro-benzyl)trisulfane (Scheme 1). The synthesis was followed by their utilization as protective ligands for a single-step approach to synthesize GNPs in an aqueous solution without using any other reducing agent.

The seven symmetrical allyl, alkyl and/or benzyl TS are generally synthesized by different methods, of which, two methods were used here. One of them was reported by Sinha *et al.*[30] involving the reaction of stannous chloride dihydrate ($SnCl_2.2H_2O$) with allyl/alkyl/benzyl halides (R-X) and sulfur powder (S_8) in presence of catalytic cupric chloride ($CuCl_2.2H_2O$) in THF:DMSO (2:1 v/v) refluxed at 70–80 °C giving the desired trisulfides (R-S-S-S-R). Reaction in the absence of $CuCl_2.2H_2O$ showed less than 5% conversion. However, the major problem with this method is the formation of too many undesired side products, and the unpredictability of the desired product. Another efficient method for the synthesis of the TS compounds was reported by Ren *et al.*[38] where alkyl or allyl halide reacts with saturated solution of sodium thiosulfate ($Na_2S_2O_3.5H_2O$) at 50–60 °C for several hours followed by the addition of 30 mL of sodium sulfide ($Na_2S.5H_2O$) solution at room temperature (Scheme 2). The reaction time and carbon chain number have a significant effect on the yield of the compounds. It was noticed that an increase in the number of carbon chain significantly increases the reaction time and lowers the yield of the compound. Although Ren and co-workers reported only the synthesis of symmetrical aliphatic alkyl or allyl TS, herein, we have adopted their route to synthesize different aromatic compounds as well.

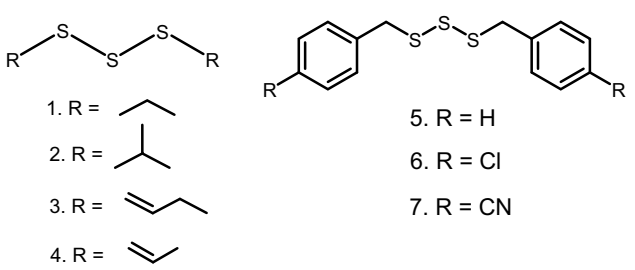

Scheme 1. Chemical structures of allyl/alkyl/benzyl trisulfide derivatives.

Of the possible isomeric forms of thiosulfate, "i" and "ii", the chemical behavior of sodium-S-alkyl/aryl-thiosulfates, known as Bunte salt (Scheme 3)[39] is compatible only with "ii" since $S_2O_3^{2-}$ should contain different nucleophilic centers and the nucleophilic strength should be greatest on the S atom due to its high electron affinity. Na_2S gives S^{2-} that acts as a nucleophile and possibly attacks the central S^{6+} of the Bunte salt. This breaks the d-p or d-d π-bonds, further stabilizing the S-S σ-bond (catenation property of S), which in turn attacks other R-S_2O_3Na followed by poly-condensation to form the disulfide bridged derivatives. Hence, the assigned TS derivatives 1, 2, 3, 5 and 6 were synthesized by the method described by Ren et al. depending upon the commercial availability of the halides.

3.2 *Preparation of GNPs with the DATs*

Preparation of the TS-GNPs was carried out with different volumes of the TS derivatives to monitor the progress of the reaction. Importantly, here the TSs (as ligand) act as both reducing agent and stabilizer of the GNPs. The change in color of the synthetic solution suggests the formation of TS-GNPs, which was further monitored by the absorption spectra. To compare the results using the TS ligands, we prepared GNPs conventionally by reducing $HAuCl_4$ with Vitamin-C (Vit-C-GNP). The TS-based reactions were monitored by the change in the absorption spectra at regular intervals for 20 mins. The TS derivatives 1, 2, 5 and 6 did not show the development of any characteristic surface plasmon resonance (SPR) absorption band of GNP

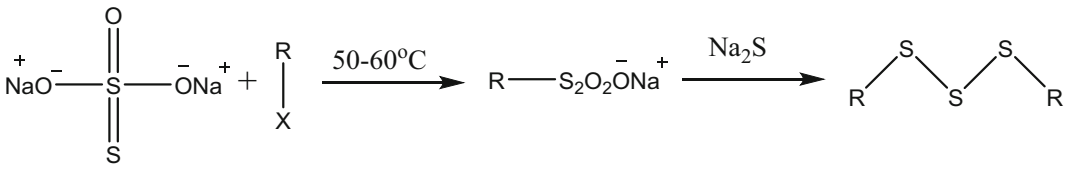

Scheme 2. Schematic diagram for the synthesis of the TS.

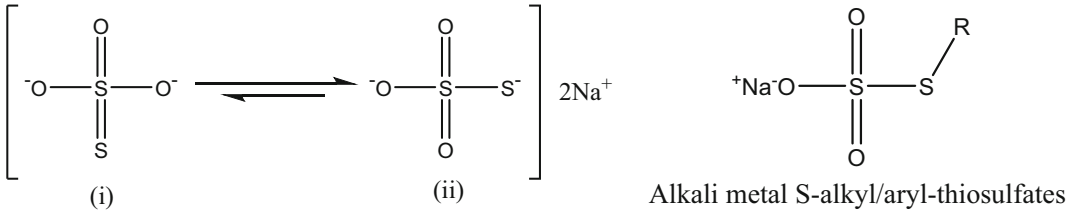

Scheme 3. The possible isomers of thiosulfate and structure of Bunte salt.

(Figure 1). However, with the TS ligand 3 (1,3-di(but-1-ene)trisulfane), we observed a distinct formation of the characteristic SPR band at 580 nm with time. This clearly shows the formation of butene-TS-GNP. Interaction of ligand 3 with the GNPs was confirmed from IR spectroscopy as well (Figures S1 and S2, SI).

We found that only the butene-TS (ligand 3) helps forming the desired GNPs and the other trisulfane derivatives fail. To look deeper into the problem, we determined the changes with varying concentrations of ligand 3. For this, 50 mM solution of ligand 3 was added to 10 mL boiling gold salt solution, in steps of 6–15 µL and the formation of GNP was monitored from the changes in the absorption spectrum (Figure 2). On addition of the ligand up to 7 µL, the SPR signal appeared at 580 nm. However, on further addition of the protecting ligand 3, the SPR band shifted to higher energy. Hence, we estimated that the addition of 8–10 µL of ligand 3 solution probably produces smaller GNPs stabilized by a decent number of the protecting ligands. However, at even higher concentrations, the GNPs lose optical density. We picked up the three critical volumes (or concentrations), typically 7 µL, 10 µL and 15 µL corresponding to 35, 50 and 65 µM of ligand 3, respectively, to characterize the butene-TS-GNPs further.

3.3 *Characterization of the synthesized GNPs*

For physical characterization of the newly formed butene-TS-GNPs, we measured the hydrodynamic diameters and the surface charges at the three different chosen concentrations. In our experimental condition, the average hydrodynamic diameters of the butene-TS-GNP were found to be ~150 nm for all the concentrations of ligand 3 (Figure 3a). The size of the GNPs did not vary much due to change in the ligand

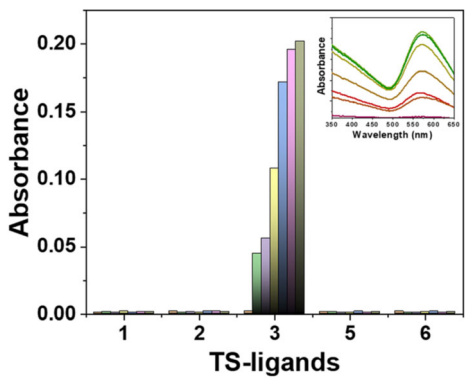

Figure 1. Change in the absorption spectra of the TS derivatives, (a) 1, (b) 2, (c) 5 and (d) 6 with time (each column is showing different times from 1–20 mins) signifying no formation of GNP due to the reaction.

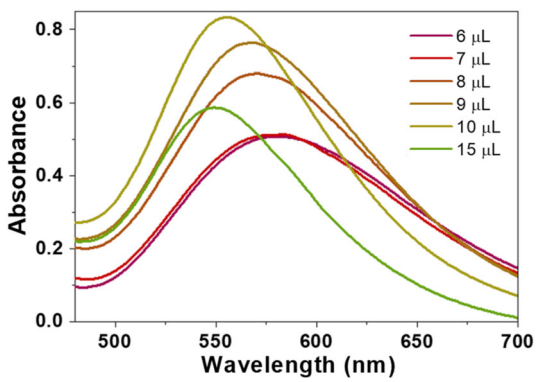

Figure 2. Change in the absorption spectra of the TS ligand 3 on addition to the gold salt solution in steps.

concentration. Poly-dispersity index (PDI) represents the heterogeneity in the size of the particles. The PDI values of 0.376, 0.324 and 0.304 for 7, 10 and 15 μL addition, respectively, suggest that the particles are more or less homogeneously distributed in solution. The surface charge and conductivity of the butene-TS-GNPs were found to be (a) -44.5 mV and 0.131 mS/cm for 7 μL addition, (b) -45.8 mV and 0.203 mS/cm for 10 μL addition, and (c) -49.1 mV and 0.144 mS/cm for 15 μL addition, respectively (Figure 3b). While the magnitude of the negative surface charge increases with an increase in the concentration of the added ligand, the conductivity increases for the 10 μL ligand addition compared to the other two values. This is consistent with the observed absorption spectral changes. The variations can be attributed to the difference in the core size of the metal.

To measure the size distribution of the butene-TS-GNPs on the addition of the varying concentrations of 3 during synthesis, we took their TEM images (Figure 4). High resolution TEM (HRTEM) images show that the distance between two lattice planes in the butene-TS-GNPs is ~0.20 nm that matches well with the (111) lattice spacing of face centered cubic (fcc) Au and confirms a high degree of crystallinity of the NCs. The presence of Au in the NPs was confirmed from electron dispersive spectroscopy (EDS). The sizes of the GNPs were 5 nm and 3 nm on adding 35 and 50 μM of ligand 3 which corroborate nicely with the absorption spectra.

3.4 *Theoretical analysis on the selectivity of the DATs*

To interpret this behavior and the speciality of ligand 3 over the others, we calculated the frontier molecular orbitals (FMOs) of the ligands using density functional theory (DFT) with B3LYP/6-31G* basis set (Figure 5). It was observed that ligand 3 has a curved structure with a proper interstitial void that probably facilitates it to fit appropriately on the surface of the developing GNPs. Moreover, the structure of ligand 3 helps the molecule to have an intramolecular dp–π electron transfer from the C=C to the vacant d-orbitals of sulfur. As a result, the sulfur atom attains the electron density and helps further to reduce Au(III) to Au(I). Thus, ligand 3 acts both as a good protecting as well as reducing agent in the GNP synthesis. The shape of the other TS-ligands differ from that of ligand 3 and hence they are improbable to act as suitable protecting groups for the GNPs. In ligand 1, i.e., 1,3-di(n-propyl)trisulfane, the reducing power of S could not increase due to the simple aliphatic chains. In 2, the bulky Me-groups in the 1,3-di(isobutyl) chains prohibited the reducing center to approach the gold atoms. For 5 and 6, calculations show that the electron density was distributed all over the molecule in HOMO and the two benzyl rings tend to always maintain their aromaticity. As a consequence, probability of π-electron transfer to the S-atom decreases. The above results explain the reason for 3 to behave well as protecting and reducing agent for the GNPs.

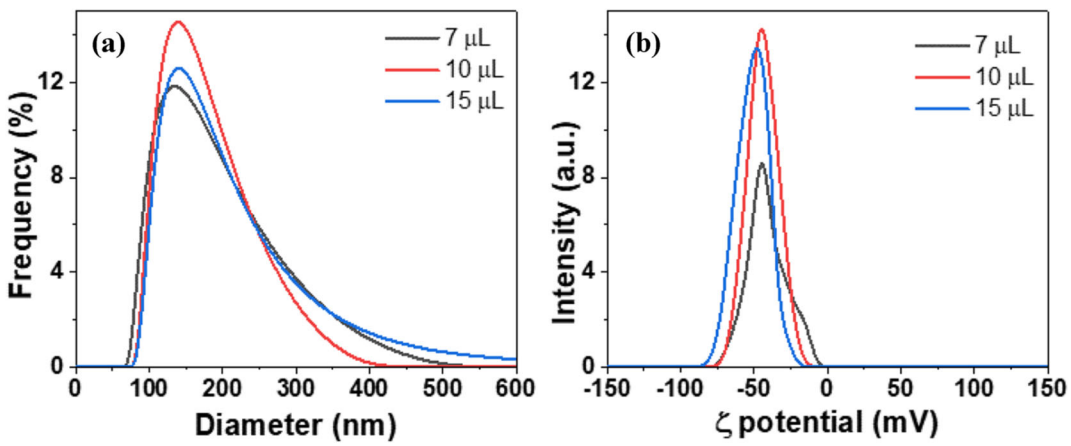

Figure 3. (a) Particle size distribution of butene-TS-GNP prepared by adding 7 μL, 10 μL and 15 μL of 50 mM butene-TS ligand to 10 mL of the gold salt solution, as measured by DLS; (b) shows the corresponding plots for the zeta (ζ) potentials.

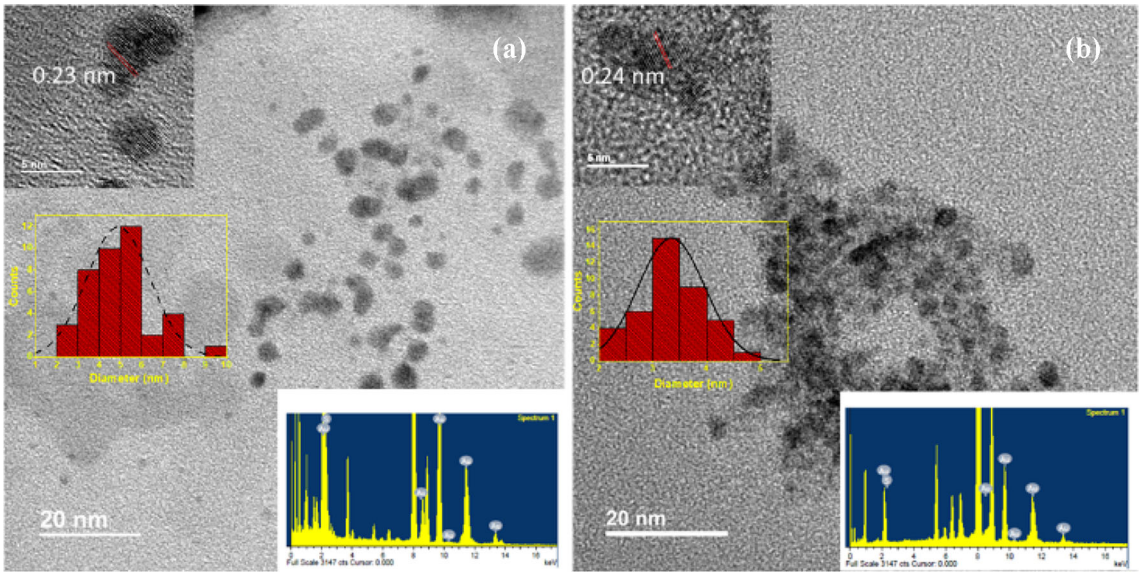

Figure 4. TEM micrographs for particle size distribution of butene-TS-GNP prepared by adding (a) 7 μL and (b) 10 μL of 50 mM butene-TS ligand to 10 mL of the gold salt solution. The insets show the interplanar distances and size distribution histograms for the samples. Electron dispersive spectroscopy (EDS) confirms the presence of Au.

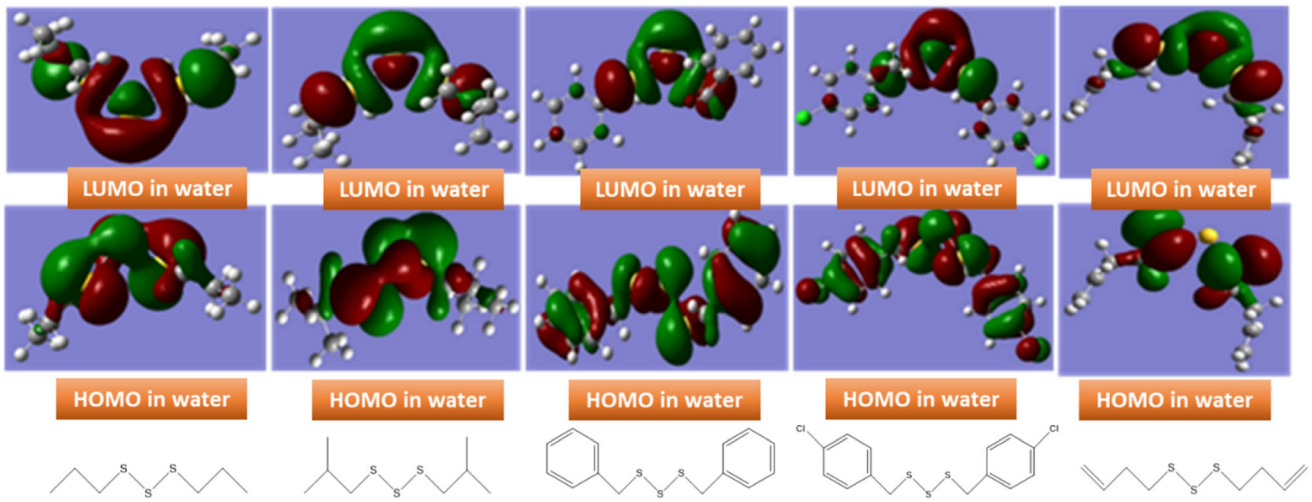

Figure 5. The calculated FMOs of the synthesized TS-ligands.

4. Conclusions

The present report has produced a detailed view on the synthesis of organosulfur compound induced GNPs (TS-GNPs). In the process, to optimize the right ligand to produce the GNPs, we synthesized a series of DATS derivatives. Interestingly, only 1,3-di(but-1-ene)trisulfane could effectively reduce chloroauric acid and protect the synthesized GNPs. Theoretical calculations showed that the sulfhydryl group of the trisulfide is responsible for the reduction reaction. The TS-GNPs show SPR band at 580 nm. Production of the GNPs was monitored from the development of the SPR band with time. The average hydrodynamic diameter of the GNPs ranges from 144 to 150 nm depending on the concentration of the ligand used during the synthetic process. The protecting groups being biologically important and the strong SPR property of the formed GNPs proposes a new method of synthesis of the GNPs.

Supplementary Information (SI)

The FTIR spectra of the synthesized DATS derivatives. Figures S1-S2 are available at www.ias.ac.in/chemsci.

Acknowledgements

The work was supported by the Science and Engineering Research Board (SERB), Government of India (Grant No. CRG/2018/000555). AC acknowledges SERB for his fellowship.

References

1. Park H, Park J, Lim A K L, Anderson E H, Alivisatos P H and McEuen P L 2000 Nanomechanical oscillations in a single-C60 transistor *Nature* **407** 57
2. De Franceschi S and Kouwenhoven L 2002 Electronics and the single atom *Nature* **417** 701
3. Toshima N 2008 Capped bimetallic and trimetallic nanoparticles for catalysis and information technology *Macromol. Symp.* **270** 27
4. Daniel M C and Astruc D 2004 Gold nanoparticles: assembly, supramolecular chemistry, quantum-size-related properties, and applications toward biology, catalysis, and nanotechnology *Chem. Rev.* **104** 293
5. Gao J, Gu H and Xu B 2009 Multifunctional magnetic nanoparticles: design, synthesis, and biomedical applications *Acc. Chem. Res.* **42** 1097
6. Yang G J, Qu X L, Shen M, Wang C Y, Qu Q S and Hu X Y 2007 Preparation of glassy carbon electrode modified by hydrophobic gold nanoparticles and its application for the determination of ethamsylate in the presence of cetyltrimethylammonium bromide *Sens. Actuat. B Chem.* **128** 258
7. Chiang C L 2001 Controlled growth of gold nanoparticles in AOT/$C_{12}E_4$/isooctane mixed reverse micelles *J. Colloid Interface Sci.* **239** 334
8. Yeh Y C, Creran B and Rotello V M 2012 Gold nanoparticles: preparation, properties, and applications in bionanotechnology *Nanoscale* **4** 1871
9. Dong S A and Zhou S P 2007 Photochemical synthesis of colloidal gold nanoparticles *Mater. Sci. Eng. B* **140** 153
10. Eustis S and El-Sayed M A 2006 Why gold nanoparticles are more precious than pretty gold: Noble metal surface plasmon resonance and its enhancement of the radiative and nonradiative properties of nanocrystals of different shapes *Chem. Soc. Rev.* **35** 209
11. Rosi N L and Mirkin C A 2005 Nanostructures in biodiagnostics *Chem. Rev.* **105** 1547
12. Giljohann D A, Seferos D S, Daniel W L, Massich M D, Patel P C and Mirkin C A 2010 Gold nanoparticles for biology and medicine *Angew. Chem., Int. Ed. Engl.* **49** 3280
13. Ding Y, Liu J, Wang H, Shen G and Yu R 2007 A piezoelectric immunosensor for the detection of alpha-fetoprotein using an interface of gold/hydroxyapatite hybrid nanomaterial *Biomaterials* **28** 2147
14. Mukherjee P, Bhattacharya R, Bone N, Lee Y K, Patra C R, Wang S, et al. 2007 Potential therapeutic application of gold nanoparticles in B-chronic lymphocytic leukemia (BCLL): enhancing apoptosis *J. Nanobiotechnol.* **5** 4
15. Niidome T, Yamagata M, Okamoto Y, Akiyama Y, Takahashi H, Kawano T, et al. 2006 PEG-modified gold nanorods with a stealth character for in vivo applications *J. Control. Release* **114** 343
16. Lim Z Z J, Li J E J, Ng C T, Yung L Y L and Bay B H 2011 Gold nanoparticles in cancer therapy *Acta Pharmacol. Sin.* **32** 983
17. Sztandera K, Gorzkiewicz M and Klajnert-Maculewicz B 2019 Gold Nanoparticles in cancer treatment *Mol. Pharma.* **16** 1
18. Yang C, Bromma K, Di Ciano-Oliveira C, Zafarana G, van Prooijen M and Chithrani D B 2018 Gold nanoparticle mediated combined cancer therapy *Cancer Nanotechnol.* **9** 4
19. Singh B M M, David C C, Harris-Birtill D C C, Markar S R, Hanna G B and Elson D S 2015 Application of gold nanoparticles for gastrointestinal cancer theranostics: A systematic review *Nanomedicine* **11** 2083
20. Jain P K, Huang X, El-Sayed I H and El-Sayed M A 2007 Review of some interesting surface plasmon resonance-enhanced properties of noble metal nanoparticles and their applications to biosystems *Plasmonics* **2** 107
21. Sperling R A, Gil P R, Zhang F, Zanella M and Parak W J 2008 Biological applications of gold nanoparticles *Chem. Soc. Rev.* **37** 1896
22. Hutter E and Maysinger D 2018 Gold nanoparticles and quantum dots for bioimaging *Microsc. Res. Tech.* **74** 592
23. Singh P, Pandit S, Mokkapati V R S S, Garg A, Ravikumar V and Mijakovi I 2018 Gold nanoparticles in diagnostics and therapeutics for human cancer *Int. J. Mol. Sci.* **19** 1979
24. Velsankar K, Preethi R, Jeevan Ram P S, Ramesh M and Sudhahar S 2020 Evaluations of biosynthesized Ag nanoparticles via Allium sativum flower extract in biological applications *Appl. Nanosci.* **10** 3675
25. Reda M, Ashames A, Edis Z, Bloukh S, Bhandare R and Abu Sara H 2019 Green synthesis of potent antimicrobial silver nanoparticles using different plant extracts and their mixtures *Processes* **7** 510
26. Otunola G A, Afolayan A J, Ajayi E O and Odeyemi S W 2017 Characterization, Antibacterial and antioxidant properties of silver nanoparticles synthesized from aqueous extracts of Allium sativum, Zingiber officinale, and Capsicum frutescens *Pharmacogn. Mag.* **13** S201
27. Von White II G, Kerscher P, Brown R M, Morella J D, McAllister W, Dean D and Kitchens C L 2012 Green synthesis of robust, biocompatible silver nanoparticles using garlic extract *J. Nanomater.* 730746
28. Lawson L D and Hunsaker S M 2018 Allicin bioavailability and bioequivalence from garlic supplements and garlic foods *Nutrients* **10** 812
29. Meléndez-Villanueva M A, Morán-Santibañez K, Martínez-Sanmiguel J J, Rangel-López R, Garza-Navarro M A, Rodríguez-Padilla C, et al. 2019 Virucidal activity of gold nanoparticles synthesized by green chemistry using garlic extract *Viruses* **11** 1111
30. Rastogi L and Arunachalam J 2013 Green synthetic route for the size controlled synthesis of biocompatible gold nanoparticles using aqueous extract of garlic (Allium sativum) *Adv. Mater. Lett.* **4** 548

31. Ateeq M, Shah M R, Ali H, Kabir N, Khan A and Nadeem S 2015 Hepatoprotective and urease inhibitory activities of garlic conjugated gold nanoparticles *New J. Chem.* **39** 5003
32. Yulizar Y, Ariyanta H A and Abdurrachman L 2017 Green synthesis of gold nanoparticles using aqueous garlic (Allium sativum L.) extract and its interaction study with melamine *Bull. Chem. React. Eng. Catal.* **12** 212
33. Shi X, Li D, Xie J, Wang S, Wu Z and Chen H 2012 Spectroscopic investigation of the interactions between gold nanoparticles and bovine serum albumin *Chin. Sci. Bull.* **57** 1109
34. Jiang Z L, Feng Z W, Li T S, Li F, Zhong F X, Xie J Y and Yi X H 2001 Resonance scattering spectroscopy of gold nanoparticle *Sci. China Ser. B Chem.* **44** 175
35. Borkowska A, Knap N and Antosiewicz J 2013 Diallyl trisulfide is more cytotoxic to prostate cancer cells PC-3 than to noncancerous epithelial cell line PNT1A: A possible role of p66Shc signaling axis *Nutr. Cancer* **65** 711
36. Shigemi Z, Furukawa Y, Hosokawa K, Minami S, Matsuhiro J, Nakata S, et al. 2015 Diallyl trisulfide induces apoptosis by suppressing NF-κB signaling through destabilization of TRAF6 in primary effusion lymphoma *J. Oncol.* **48** 293
37. Yu C-S, Huang A-C, Lai K-C, Huang Y-P, Lin M-W, Yang J-S and Chung J-G 2012 Diallyl trisulfide induces apoptosis in human primary colorectal cancer cells *Oncol. Rep.* **28** 949
38. Ren F K, He X Y, Deng L, Li B H, Shin D S and Li Z B 2009 Synthesis and antibacterial activity of 1,3-diallyl-trisulfane derivatives *Bull. Kor. Chem. Soc.* **30** 687
39. Bunte H 1874 Zur constitution der unterschwefligen säure *Ber. Dtsch. Chem. Ges.* **7** 646